Talanta 113 (2013) 142–147

Contents lists available at SciVerse ScienceDirect

Talanta

journal homepage: www.elsevier.com/locate/talanta

Activity of catalase adsorbed to carbon nanotubes: Effects of carbon nanotube surface properties

Chengdong Zhang [a,b,c,*], Shuiming Luo [a,b,c], Wei Chen [a,b,c]

[a] College of Environmental Science and Engineering, Nankai University, Tianjin 300071, China
[b] Ministry of Education Key Laboratory of Pollution Processes and Environmental Criteria, Nankai University, Tianjin 300071, China
[c] Tianjin Key Laboratory of Environmental Remediation and Pollution Control, Nankai University, Tianjin 300071, China

ARTICLE INFO

Article history:
Received 27 November 2012
Received in revised form
7 March 2013
Accepted 10 March 2013
Available online 16 March 2013

Keywords:
Catalase
Carbon nanotubes
Adsorption
Surface properties

ABSTRACT

Nanomaterials have been studied widely as the supporting materials for enzyme immobilization. However, the interactions between enzymes and carbon nanotubes (CNT) with different morphologies and surface functionalities may vary, hence influencing activities of the immobilized enzyme. To date how the adsorption mechanisms affect the activities of immobilized enzyme is not well understood. In this study the adsorption of catalase (CAT) on pristine single-walled carbon nanotubes (SWNT), oxidized single-walled carbon nanotubes (O-SWNT), and multi-walled carbon nanotubes (MWNT) was investigated. The adsorbed enzyme activities decreased in the order of O-SWNT > SWNT > MWNT. Fourier transforms infrared spectroscopy (FTIR) and circular dichrois (CD) analyses reveal more significant loss of α-helix and β-sheet of MWNT-adsorbed than SWNT-adsorbed CAT. The difference in enzyme activities between MWNT-adsorbed and SWNT-adsorbed CAT indicates that the curvature of surface plays an important role in the activity of immobilized enzyme. Interestingly, an increase of β-sheet content was observed for CAT adsorbed to O-SWNT. This is likely because as opposed to SWNT and MWNT, O-SWNT binds CAT largely via hydrogen bonding and such interaction allows the CAT molecule to maintain the rigidity of enzyme structure and thus the biological function.

1. Introduction

Nanobiocatalysis, which refers to the application of enzymes immobilized on nanomaterials [1], is a rapidly growing research field. Various nanomaterials, such as nano-SiO_2, nano-TiO_2, nano-gold, carbon nanotubes (CNT), and graphene, have been explored as supporting matrices [2]. Among them CNT have attracted considerable interest because of their stability, high adsorption capacity, better retention of catalytic activity, and biocompatibility [3]. Particularly, CNT can act simultaneously as the immobilization matrix and as the electrochemical transducer, rendering wide-ranged applications in nanoelectronics, biosensor, and high-resolution imaging [4]. Moreover, CNT have an additional benefit, in that they can be surface-modified with solubilizing chains or targeting molecules, resulting in the improvement of performance and/or loading of the immobilized enzyme and enhancing their application in the biomedical field.

Both single-walled carbon nanotubes (SWNT) and multi-walled carbon nanotubes (MWNT) have been used to immobilize enzyme. SWNT are attractive for their higher surface area for protein interaction, while MWNT have the advantages of better dispersibility and lower cost. So far, most studies have focused on the development of effective immobilization methods using either SWNT or MWNT, but a few studies have attempted to understand the structural effects of CNT on enzyme loading, activity and stability [5–8], and the results indicate that the performance of enzyme–CNT complexes can be affected significantly by the structural properties of CNT. Pedrosa et al. [5] found that organophosphate hydrolase conjugated to oxidized SWNT (O-SWNT) exhibited better catalytic activity compared to that conjugated to oxidized MWNT, and they argued that this was attributable to the more uniform deposition of the enzyme on O-SWNT surface. Wang et al. [6] compared the activity and stability of covalently bonded NADH oxidase on N_α,N_α-bis(carboxymethyl)-L-lysine hydrate functionalized MWNT and SWNT. They observed that even though the two enzyme–CNT conjugates exhibited similar catalytic activities, higher enzyme loading and better stability were observed for SWNT conjugate than for MWNT conjugate. They argued that the larger surface area and higher surface curvature of SWNT allow less lateral interactions between the adjacent enzyme molecules on SWNT.

It has also been observed that the surface functionalities of CNT [7–9], in particular surface O-functionalities, can affect the

* Corresponding author at: College of Environmental Science and Engineering, Nankai University, Tianjin 300071, China. Tel./fax: +86 22 6622 9517.
E-mail address: zhangchengdong@nankai.edu.cn (C. Zhang).

0039-9140/$ - see front matter © 2013 Elsevier B.V. All rights reserved.
http://dx.doi.org/10.1016/j.talanta.2013.03.027

activities of adsorbed enzymes. For example, Mu et al. [8] found that the enzyme bound to O-MWNT exhibited weaker activity than the enzyme bound to MWNT. They proposed that MWNT bound enzymes interacted through mostly π–π stacking interactions, whereas O-MWNT interacted with enzymes mainly through negatively charged O-MWNT surface with neutral or positively charged surface residues on the protein. The stronger nanotube-binding between carbonic anhydrase and O-MWNT induced more enzyme conformational changes, thus decreasing activity. In another study, Dong et al. [9] observed that soybean peroxidase exhibited higher enzymatic activity on highly oxidized SWNT than on less oxidized SWNT. They suggested that this phenomenon may be attributed to the stronger hydrophobic interaction between the enzyme molecules and less oxidized SWNT so that more of the secondary structure was changed consequently.

To date, how the activities of enzyme–CNT conjugates are affected by the nature of adsorptive interactions between enzyme and CNT are not fully understood. To further understand the underlying mechanism, in particular the effect of surface O-functionalization on enzyme activity, we examined the adsorption properties and enzyme activities of catalase (CAT), a heme-containing metallo-enzyme, adsorbed to three different CNT. CAT was used as a model enzyme because it is one of the most common enzymes in plant and animal tissues [10], and because immobilized CAT has wide application in many industrial fields [11]. SWNT, MWNT, and O-SWNT were used as the model CNT. The adsorption affinities and mechanisms of CAT to the three CNT were examined and the controlling mechanisms were analyzed. The conformational changes of enzymes upon immobilization were studied using Fourier transform infrared (FTIR) spectroscopy and circular dichroisom (CD) spectroscopy. The correlations between CAT–CNT adsorptive interactions and enzyme activities of adsorbed CAT are discussed.

2. Materials and methods

2.1. Materials

SWNT and MWNT were purchased from Nanotech Port Co. (Shenzhen, Guangdong Province, China). A portion of the SWNT was treated with HNO_3 and H_2SO_4 mixtures (1:3 by volume) to obtain carboxylic functionalized SWNT using a previously developed method [12]. Graphite was purchased from Sigma-Aldrich. Elemental analysis, surface area and pore size distribution, and ζ potential were determined using previously reported methods [13]. Selected physical–chemical properties of the CNT are listed in Table 1.

Table 1
Elemental analysis, surface area measurements and pore size distribution of various CNT.

Adsorbent	Elemental composition[a]			Surface area[b] (m^2/g)	Pore size distribution (%)[c]		
	C%	H%	O%		Micropore (< 2 nm)	Mesopore (2–38 nm)	Macropore (> 38 nm)
SWNT	91.7	2.0	4.2	417	1	78	21
O-SWNT	82.6	1.1	8.7	310	59	41	0
MWNT	96.1	1.3	2.8	372	8	69	23

[a] Analyzed with an elemental analyzer.
[b] Surface area determined by N_2 adsorption using the Brunauer–Emmett–Teller (BET) method.
[c] Pore size distribution was calculated by the Horvath–Kawazoe function.

CAT (EC 1.11.1.6, from bovine liver) was purchased from Sigma-Aldrich. All other chemicals and solvents used were of analytical grade or higher.

2.2. Adsorption experiments

The adsorption experiments were performed using a method similar to that of Cang-Yong and Pastorin [14]. CNT (1 mg) were added to 1 ml of 0.05 M phosphate buffer at pH 7.0 and the suspension was ultrasonicated (150 W, 40 kHz) for 1 h to enhance the dispersion. The sonicated sample was dispensed into an eppendorf microcentrifuge tube, and then exposed to a freshly prepared solution of enzyme in the same buffer. The mixture was shaken on a platform shaker for 4 h at 200 rpm under room temperature. After incubation the CNT were centrifuged at 8000 rpm using a microcentrifuge and the supernatant was removed. Typically six washes were performed, and fresh buffer was added each time to remove unbound enzyme. All supernatants were analyzed for protein content using the bicinchoninic acid method (BCA) or the μBCA assay. The amount of enzyme loaded onto the CNT was determined by measuring the difference in the concentration of enzyme in solution before and after exposing it to the dispersion of CNT in buffer. In a separate test, adsorption of CAT on graphite was done using the same approach.

Effect of pH on CAT adsorption was examined by using 50 mM acetate buffer at pH 4.5, 5.0, 5.5 and 50 mM phosphate buffer at pH 6.0 6.5, 7.0, 7.5, 8.0. To study the effect of ionic strength on adsorption, the ionic strength of the solution was adjusted using NaCl to 50, 100, 150, and 200 mM at pH 7. The adsorption experiments were performed using the procedure described above. CNT concentration was maintained the same as 1 mg/mL in all experiments and the initial enzyme concentration was 0.9 mg/mL for the experiment of pH effect and 0.5 mg/mL for the experiment of ionic strength effect, respectively.

2.3. Enzyme activity assays

The activity of CAT was measured according to the method of Alptekin et al. [15], using H_2O_2 as the substrate. Briefly, the stock solution of 20 mM H_2O_2 was prepared in 50 mM phosphate buffer at pH 7.0. Then, 10 μL of free or absorbed CAT solution was added to 990 μL of 20 mM H_2O_2 in quartz cuvettes and immediately mixed by inversion. H_2O_2 depletion was examined at 240 nm using a UV–vis spectrometer every 10 s for over a period of 90 s. One unit is defined as the amount of CAT required to decompose 1 μmol of H_2O_2 per min at 25 °C at pH 7.0. The stock solution of adsorbed enzyme was prepared by resuspending CAT–CNT conjugate in 1 ml of 50 mM phosphate buffer at pH 7.0. The presence of 10 μg/mL of CNT in the solution will not interfere with activity measurement [16].

Kinetic parameters of the free CAT and CAT adsorbed to CNT were investigated at various concentrations (2–25 mM) of H_2O_2 (in 50 mM phosphate buffer at pH 7.0) as the substrate. The enzyme loading was maintained approximately the same for all immobilized enzyme at 240 μg/mg. The Michaelis–Menten kinetic is defined as

$$v = \frac{V_{max}[S]}{K_m + [S]} \quad (1)$$

where v is the reaction rate (mmol/min), $[S]$ is the concentration of substrate (mmol/L), V_{max} (mmol/min) is the maximum rate achieved by the system at maximum (saturating) substrate concentrations, and K_m (Michaelis–Menten constant, mmol/L) is the substrate concentration at which the reaction rate is half of V_{max}. K_m and V_{max} were determined from the Lineweaver–Burk double

reciprocal plots as given below:

$$-\frac{1}{v}=\frac{1}{V_{max}}+\frac{K_m}{V_{max}}\frac{1}{[S]} \quad (2)$$

It is well known that V_{max} reflects the intrinsic characteristics of the immobilized enzyme and can be affected by diffusion constrains, while K_m reflects the effective characteristics of the enzyme and depends upon both partition and diffusion effects [15].

2.4. Secondary structural analysis using FTIR and CD

After adsorption the sample was lyophilized using a freeze dryer (LGJ-18, Beijing Songyuan Scientific Co.). The lyophilized CAT–CNT composite (1 mg) was then ground with about 50 mg of FTIR grade KBr to form a homogeneous powder, which was then used to form a pellet for FTIR analysis (Bruker TENSOR 27 apparatus, Germany). All of the spectra were taken via the transmission mode between 4000 and 400 cm^{-1} and the IR system was continuously purged with dry air to reduce the interference of water vapor and carbon dioxide. Spectra were obtained at 4 cm^{-1} resolution with 16 scans.

The CD spectra were obtained using a JASCO-715 spectropolarimeter to evaluate the structural change of CAT induced by the addition of CNT. The far UV region was scanned between 200 and 250 nm with an average of three scans and a bandwidth of 2.0 nm at 25 °C. CAT in pH 7.0 phosphate buffer was mixed with various CNT, giving final concentrations of CAT and CNT to be 30 μg/mL and 50 mg/L, respectively. Each suspension was allowed to equilibrate for 20 min, and CD spectra were measured in a 1-cm light path cell. Simultaneously, the reagent blank without CAT was measured for correcting the mean residue ellipticity (MRE) of CAT. The relative contents of secondary structures, including α-helix, β-pleated sheet, β-turn and random coil, were calculated.

3. Results and discussion

3.1. Adsorption mechanisms of CAT to different CNT

The adsorption results of CAT on the three different CNT are shown in Fig. 1. The concentration ranges for the isotherms in Fig. 1 were chosen to cover the concentrations of enzyme used in the enzyme activity experiments. The adsorption data were normalized for surface area and were fitted with the Freundlich isotherm: $q=K_F C_w^n$, where q (μg/m^2) is the surface area-normalized equilibrium concentration of CAT on a CNT; C_w (μg/L) is the equilibrium concentration of CAT in the aqueous solution,

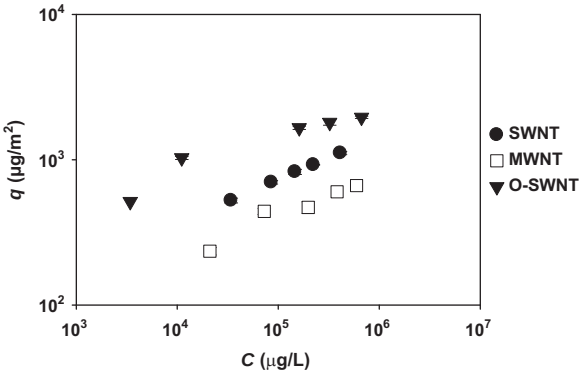

Fig. 1. Adsorption isotherms plotted as adsorbed concentration (q) versus aqueous-phase equilibrium concentration (C) of CAT to different CNT samples at pH 7.0 in 0.05 M phosphate buffer. Error bars, in some cases smaller than the symbols, represent standard deviations of the three measurements.

K_F (μmol^{1-n} L^n/kg) is the Freundlich affinity coefficient; and n (unitless) is the linearity index. The fitting parameters are summarized in Table S1. In general the Freundlich model provided reasonably good fits to the data. All three isotherms are highly nonlinear (the n values are all less than 0.30), indicating heterogeneous distributions of adsorption sites. The surface area-normalized adsorption affinities of CAT on the three CNT followed the order of O-SWNT > SWNT > MWNT (as indicated by the relative positions of the isotherms in Fig. 1). For example at the same initial enzyme concentration of 1.3 mg/mL, the enzyme loadings would be 1880 μg/m^2 for O-SWNT, 1067 μg/m^2 for SWNT and 837 μg/m^2 for MWNT.

It has been proposed that the non-covalent adsorption of enzymes to CNT is driven mainly by the hydrophobic effect, and by electrostatic interaction and hydrogen bonding (H-bonding) between enzyme and CNT [3]. The adsorption of CAT to SWNT and MWNT is controlled primarily by the hydrophobic effect [3,10]. The stronger adsorption affinity to SWNT than that to MWNT may be because that MWNT are more microporous than SWNT (see size distribution in Table 1) and the surface area associated with micropores is expectedly inaccessible to the large sized CAT (7 nm × 8 nm × 10 nm) due to size exclusion.

The surface-oxidized CNT, O-SWNT, has markedly higher oxygen content (8.7%) than the two pristine CNT. These surface O-contents are mainly carboxylic, phenolic and hydroxyl functional groups [17]. Accordingly, H-bonding (e.g., between the carboxylic and amino groups of CAT and carboxylic and hydroxyl groups of O-SWNT) is likely an important mechanism controlling the CAT–O-SWNT interaction. To verify the importance of this mechanism, we examined the effect of pH and ionic strength on the adsorption of CAT on O-SWNT. As shown in Fig. 2a, on O-SWNT highest enzyme loading was observed when pH was equal to or below 5.4, and significantly inhibited adsorption was observed when pH increased from 5.4 to 8. When pH is below the isoelectric point value (pI) of CAT (5.4), some segments of CAT (for instance, carboxylic and amino groups) can be protonated, which favors H-bonding with the O-functional groups on O-SWNT surface. Increasing pH can result in deprotonation of functional groups of both CNT and CAT, and therefore, significantly impede H-bonding. The mechanism of H-bonding is further verified with the FTIR analysis data (discussed later). Note that both SWNT and MWNT contain small amount of oxygen (Table 1). Thus, H-bonding can also be a viable mechanism for the adsorption of CAT to these two CNT, but to a much lesser degree; this is consistent with similar but much less significant pH dependency observed for the adsorption of CAT to SWNT/MWNT than to O-SWNT (Fig. 2a).

Data shown in Fig. 2a indicate that electrostatic interactions possibly cannot make as significant contribution to overall adsorption as H-bonding. If the electrostatic interaction were an important mechanism for adsorption, enhanced adsorption should be expected (within the neutral pH range) with an increasing concentration of cations, which decreases the electrostatic repulsion between the negatively charged CAT molecules and also negatively charged surfaces of CNT (see ζ potential measurements in Fig. S1) due to the shielding effects. However, as shown in Fig. 2b at neutral pH increasing concentration of NaCl from 50 to 200 mM only resulted in slightly enhanced adsorption on SWNT and even inhibited adsorption on O-SWNT.

The nature of adsorption interactions between CAT and CNT can be further understood with the FTIR data (Fig. 3). The introduction of O-functionalities on O-SWNT was confirmed by the increased oxygen content in the elemental analysis and the presence of adsorption peak of –OH, C–O, and C=O in the FTIR analysis (Fig. 3a). In Fig. 3b the region from 1000 to 420 cm^{-1} corresponding to the bending mode of the substituted benzene ring exhibits three intense bands centered at 985, 864, 534 cm^{-1} for CAT–SWNT

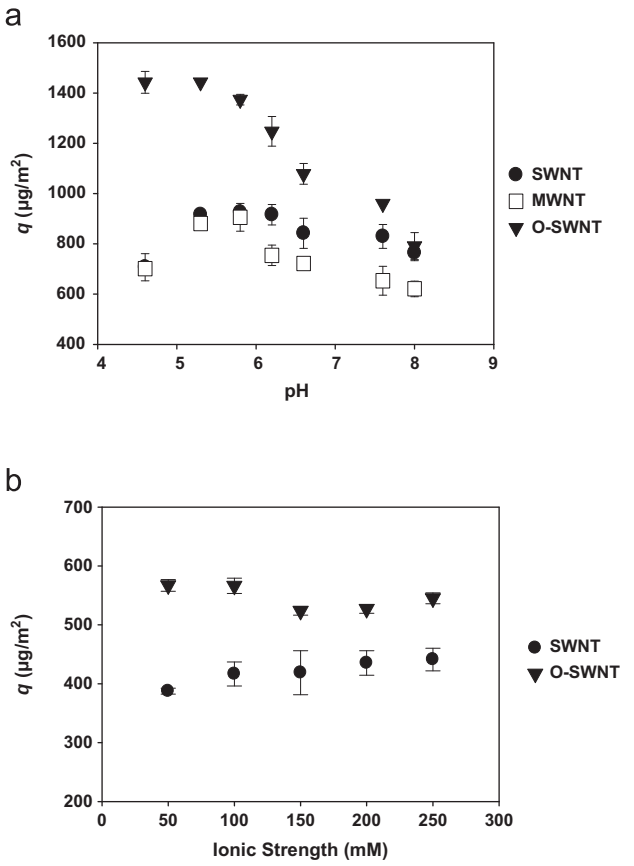

Fig. 2. Effect of pH (a) and ionic strength (b) on adsorption affinity of CAT to different CNT samples. The CNT concentration was 1 mg/mL in all cases and the initial enzyme concentration was 0.9 mg/mL for the pH effect experiments and 0.5 mg/mL for the ionic strength effect experiments.

and at 989, 860, 530 cm^{-1} for CAT–O-SWNT. In comparison with the featureless baselines of O-SWNT and SWNT in this region (Fig. 3a), the appearance of these characteristic peaks indicates strong interactions between the sidewall of the CNT and CAT, which was likely due to the hydrophobic interactions between the sidewall of CNT and some hydrophobic residues, in particular the aromatic residues of CAT [18]. Moreover, the region from 3200 to 3600 cm^{-1} corresponds to the –OH stretch mode, and the red shift of the CAT–O-SWNT (3296 cm^{-1}) compared with free CAT and CAT–SWNT (both exhibit one intense feature band centered at 3284 cm^{-1}), indicates strongly of H-bonding formation.

3.2. Enzyme activity of CAT adsorbed to CNT

The enzyme activities of CAT adsorbed to all three CNT are considerably lower than that of free CAT. The CAT–CNT conjugates generally followed the conventional Michaelis–Menten enzyme kinetics with H_2O_2 as the substrate. The K_m and V_{max} values were calculated from the Linerweave–Burk plots (Fig. S2). As shown in Table 2, K_m and V_{max} values of the free CAT are 116.3 mM and 34.4×10^3 μmol H_2O_2 mg $protein^{-1}$ min^{-1}, respectively, and are comparable with the values reported in the literature [11,19]. The K_m and V_{max} values of the three CAT–CNT conjugates are appreciably lower than the respective values of the free CAT—the K_m values are 80.6%, 27.0%, and 73.6% lower for CAT immobilized on SWNT, O-SWNT, and MWNT respectively; the V_{max} values are 34.3, 6.3, and 43.1 times lower. Lower K_m values for solid-immobilized enzymes have been reported previously [20] and were attributed to the conformation change of the immobilized enzyme and to a higher concentration of substrate on the enzyme/matrix surface due to the fact that the porous support might serve as a nucleation site for H_2O_2 [15], thereby decreasing the diffusion resistance. The decrease of V_{max} upon the immobilization process was reported by many researchers [11,15], which may be because of the conformational changes of CAT.

An interesting observation is that CAT adsorbed to O-MWNT exhibited markedly greater enzyme activities compared with CAT adsorbed to SWNT or MWNT (see V_{max}/K_m values in Table 2 and retained activities in Fig. S3). This indicates that the nature of enzyme–CNT interactions—as affected by the surface functionality of CNT—affects not only adsorption affinity, but also the activities of adsorbed enzyme. As mentioned above, H-bonding is a significant adsorption enhancement mechanism for the adsorption of CAT to O-SWNT, whereas for the adsorption of CAT to the pristine SWNT and MWNT, the relative contribution of H-bonding to the overall adsorption is much smaller (for the pristine CNT, the hydrophobic effect is likely the predominant mechanism controlling CAT–CNT interactions; this is consistent with other studies involving enzyme and pristine CNT [13,16]). The formation of hydrogen bonds could affect enzyme conformation and activity in two ways. First, when enzymes adsorb to CNT surfaces via the hydrophobic effect (mostly through hydrophobic residues of CAT), the hydrophobic residues (which are normally buried within the protein molecule) may become exposed to the surface, causing structure denaturation [21]. However, H-bonding formation may decrease the hydrophobic effect induced denaturation by orientating more polar and charged amino acids in the proximity of the nanotubes. Wijaya et al. [22] performed semi-empirical simulation of the SWNT–bovine serum albumin (BSA) interaction. The results show that there is 67.7% hydrophobic residues from BSA in the surroundings of pristine SWNTs in comparison with 51.2% of hydrophobic residues in the neighbor of carboxylated SWNT. Second, H-bonding formation between peptide units and polar groups of O-SWNT could stabilize the secondary structure by acting as a rigid multifunctional crosslinker [23] (see more discussion on the CD spectroscopy data below).

We observed a slightly greater enzyme activity of CAT adsorbed to SWNT than on MWNT. This is interesting considering that SWNT and MWNT have the same atomic surface structures whereas the only major difference is in their diameters—1 nm for SWNT and 15–30 nm for MWNT in our study. As a result, SWNT have higher surface curvature (2 nm^{-1}) in comparison with MWNT (0.13–0.07 nm^{-1}). It is generally accepted that highly curved surfaces are unfavorable for enzyme denaturation and suppress lateral interactions between adjacent adsorbed enzymes, and therefore, allowing adsorbed enzyme to maintain structural integrity and catalytic activity [8]. To further verify that the difference in enzyme activities between CAT–SWNT and CAT–MWNT is due to the surface curvature, additional test was conducted using graphite as the supporting matrix—the flat surface of graphite is expected to promote multiple contacts between enzyme and the matrix, and consequently, lead to considerable changes of structure and catalytic function. As expected, at the same enzyme loading the retained activity of immobilized CAT decreased in the order of O-SWNT > SWNT > MWNT > graphite (Fig. S3). The effects of surface curvature on the lateral interactions between two adsorbed enzymes are depicted in Fig. 4.

3.3. Secondary structure of CAT adsorbed to CNT by FTIR and CD analyses

To verify the hypothesis that the differences in enzyme activity among CAT adsorbed to the different CNT were mainly caused by the differences in CAT structure induced upon the adsorptive interactions, FTIR and CD analyses were conducted. Among the different bands of protein, the amide I in region 1600–1700 cm^{-1}

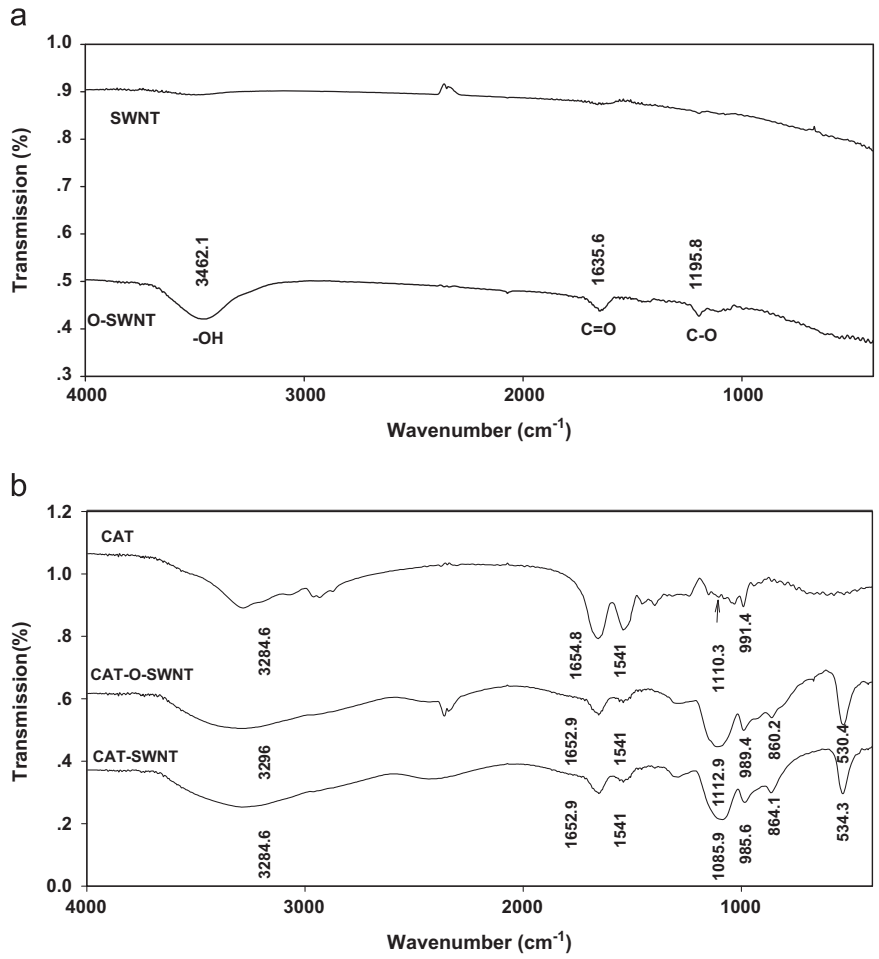

Fig. 3. FTIR spectra of (a) SWNT and O-SWNT; and (b) free CAT, CAT adsorbed to SWNT (CAT–SWNT), and CAT adsorbed to O-SWNT (CAT–O-SWNT).

(mainly C═O stretch) has a relationship with the secondary structure of protein. As shown in Fig. 3, a shift in amide I from 1654.8 cm^{-1} (for free CAT) to 1652.9 cm^{-1} (for CAT adsorbed to O-SWNT and SWNT) with a loss of intensity indicates change of the secondary structure and decrease of enzymatic activity. Note that different regions of the amide I band are contributed by different secondary structural elements: 1620–1645 cm^{-1} by β-sheet, 1645–1652 cm^{-1} by random coil, 1652–1662 cm^{-1} by α-helix, and 1662–1690 cm^{-1} by turn [24]. A closer look at this region (Fig. S4) shows different alteration patterns between CAT–O-SWNT and CAT–SWNT. The subtle structure change will be further analyzed with the CD spectroscopy. The changes in FTIR and CD spectra are consistent with the literature studies [24,25], and indicate the secondary structural changes of enzyme.

The absorbance intensity of the amide II band in the region 1500–1600 cm^{-1} (C–N stretch coupled with the N–H bending mode) has been reported to be proportional to the amount of the protein absorbed on a surface [24]. There were no position shifts for the amide II N–H bands centered at 1541 cm^{-1} while significant decreases in intensities were observed for CAT–O-SWNT and CAT–SWNT. This indicates that CAT were attached to CNT surfaces and the micro-environments of amide II bond were not affected, which explains why certain enzymatic activities were maintained. However, for CAT–MWNT (Fig. S5) position shifts were observed for both amide I and II bands and peak intensity decreased dramatically, which clearly demonstrates the significant change of secondary structure and loss of catalytic activity.

To further characterize the subtle changes of secondary structure of CAT upon adsorptive interactions with O-SWNT and SWNT, the CD spectra were obtained (Fig. 5). Compared with O-SWNT, SWNT have different effects on the secondary structure (Table 3). In the presence of SWNT, the α-helix content decreased from 26.0% to 22.8%, and the β-sheet content decreased from 12.0% to 10.9%. The decrease of α-helix indicates unfolding of enzyme on SWNT surface. The decrease of β-sheet and increase of random coil and turn suggest that enzyme interaction with the surface disrupts H-bonding within the β-sheet structure, leading to the formation of more flexible structure [21]. Interestingly, distinctively different patterns were observed for O-SWNT, in that the content of α-helix was almost unchanged and the content of β-sheet increased to 15.3%. The results indicate that due to the H-bonding formation the surface of O-SWNT is able to act as a template to induce the refolding of the protein with the formation of

Table 2
Kinetic constants [maximum rate (V_{max}) and the Michaelis–Menten constant (K_m)][a] and catalytic efficiency (V_{max}/K_m) of free and adsorbed CAT.

Enzyme form	V_{max} (μmol H_2O_2 mg^{-1} min^{-1})	K_m (mM)	V_{max}/K_m (g^{-1} min^{-1})
Free CAT	$34.4 \times 10^3 \pm 519$	116.3 ± 10.2	295.8
Adsorbed to SWNT	$9.7 \times 10^2 \pm 27$	22.5 ± 3.5	43.1
Adsorbed to O-SWNT	$4.7 \times 10^3 \pm 315$	84.8 ± 5.5	55.4
Adsorbed to MWNT	$7.8 \times 10^2 \pm 50$	30.7 ± 7.8	25.4

[a] The K_m and V_{max} values were calculated from Linerweave–Burk plots in SI Fig. 2.

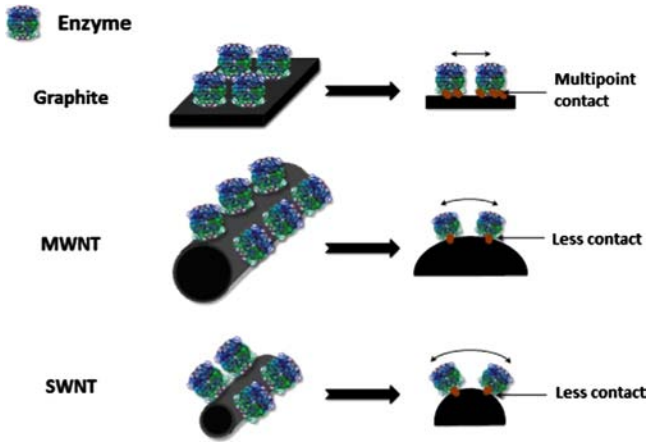

Fig. 4. Schematic depiction of the reduced lateral interactions between enzyme molecules on the surface with higher curvature.

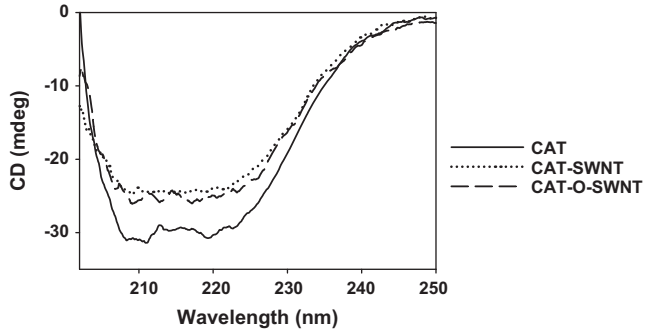

Fig. 5. Molar ellipticity CD spectra of free CAT, CAT adsorbed to SWNT (CAT–SWNT), and CAT adsorbed to O-SWNT (CAT–O-SWNT). Concentration of O-SWNT or SWNT, when present, was 50 mg/L (pH 7.0 in 0.05 M phosphate buffer).

Table 3
Calculated secondary structure of CAT with different CNT in accordance with Fig. 5.

	α helix (%)	β sheet (%)	β turn (%)	Random coil (%)
Free CAT	26.0	12.0	20.6	41.4
Adsorbed to SWNT	22.8	10.9	23.0	43.3
Adsorbed to O-SWNT	25.5	15.3	15.6	43.6

CAT concentration was 30 mg/L and CNT concentration was 50 mg/L in all cases. Standard deviation was less than 1% in all cases.

new β-sheet structure. Because of that, the secondary structure of CAT was more rigid on O-SWNT, and that is likely the reason why the enzyme retained greater activity than that on SWNT. Further studies that apply the molecular simulation approach to examine the refolding of protein induced by surface O-functionalities of CNT would be useful to further verify the mechanisms proposed in this study.

4. Conclusions

A better understanding of the mechanisms controlling the interactions between CNT and biomolecules is the basis for environmental, biological and medical applications of CNT. Our results have shown that surface functionality of CNT could significantly affect the nature of adsorptive interactions between CAT and CNT, thereby affecting the secondary structure and biological function of enzyme. Additionally, enzyme activity is also influenced by the unique surface curvature of the nanomaterials. Therefore, by tuning the stereochemistry and surface properties of CNT, the enzyme-binding capability can be regulated and bioactivity improved, optimizing their potential application in nanobiosensor and nanobiomedicine.

Acknowledgments

This Project was supported by the National Natural Science Foundation of China (Grants 81250003 and 21237002), and the Tianjin Municipal Science and Technology Commission (Grant 09JCYBJC26900).

Appendix A. Supplementary material

Supplementary data associated with this article can be found in the online version at http://dx.doi.org/10.1016/j.talanta.2013.03.027.

References

[1] I.V. Pavlidis, T. Vorhaben, T. Tsoufis, P. Rudolf, U.T. Bornscheuer, D. Gournis, H. Stamatis, Bioresource Technol. 115 (2012) 164–171.
[2] S.A. Ansari, Q. Husain, Biotechnol. Adv. 30 (2012) 512–523.
[3] W. Feng, P. Ji, Biotechnol. Adv. 29 (2011) 889–895.
[4] S.K. Vashist, D. Zheng, K. Al-Rubeaan, J.H. Luong, F.S. Sheu, Biotechnol. Adv. 29 (2011) 169–188.
[5] V.A. Pedrosa, S. Paliwal, S. Balasubramanian, D. Nepal, V. Davis, J. Wild, E. Ramanculov, A. Simonian, Colloids Surfaces B: Biointerfaces 77 (2010) 69–74.
[6] L. Wang, R. Xu, Y. Chen, R. Jiang, J. Mol. Catal. B: Enzymatic 69 (2011) 120–126.
[7] B. Zhang, Y. Xing, Z. Li, H. Zhou, Q. Mu, B. Yan, Nano Lett. 9 (2009) 2280–2284.
[8] Q. Mu, W. Liu, Y. Xing, H. Zhou, Z. Li, Y. Zhang, L. Ji, F. Wang, Z. Si, B. Zhang, B. Yan, J. Phys. Chem. C 112 (2008) 3300–3307.
[9] C. Dong, A.S. Campell, R. Eldawud, G. Perhinschi, Y. Rojanasakul, C.Z. Dinu, Appl. Surf. Sci. 264 (2013) 261–268.
[10] J.L. Felhofer, J.D. Caranto, C.D. Garcia, Langmuir: ACS J. Surf. Colloids 26 (2010) 17178–17183.
[11] S.S. Tukel, O. Alptekin, Process Biochem. 39 (2004) 2149–2155.
[12] W. Chen, L. Duan, L. Wang, D. Zhu, Environ. Sci. Technol. 42 (2008) 6862–6868.
[13] L. Ji, W. Chen, J. Bi, S. Zheng, Z. Xu, D. Zhu, P.J. Alvarez, Environ. Toxicol. Chem./SETAC 29 (2010) 2713–2719.
[14] J.T. Cang-Rong, G. Pastorin, Nanotechnology 20 (2009) 255102.
[15] Ö. Alptekin, S.S. Tükel, D. Yıldırım, D. Alagöz, J. Mol. Catal. B: Enzymatic 64 (2010) 177–183.
[16] S.S. Karajanagi, A.A. Vertegel, R.S. Kane, J.S. Dordick, Langmuir: ACS J. Surf. Colloids 20 (2004) 11594–11599.
[17] W. Chen, L. Duan, D. Zhu, Environ. Sci. Technol. 41 (2007) 8295–8300.
[18] P. Bertoncini, O. Chauvet, J. Phys. Chem. B 114 (2010) 4345–4350.
[19] U. Chatterjee, A. Kumar, G.G. Sanwal, J. Ferment. Bioeng. 90 (1990) 429–430.
[20] N. Tüzmen, T. Kalburcu, A. Denizli, Process Biochem. 47 (2012) 26–33.
[21] A.A. Shemetov, I. Nabiev, A. Sukhanova, ACS Nano 6 (2012) 4585–4602.
[22] I.P.Mahendra Wijaya, S. Gandhi, T.Ju Nie, N. Wangoo, I. Rodriguez, G. Shekhawat, C.R. Suri, S.G. Mhaisalkar, Appl. Phys. Lett. 95 (2009) 073704.
[23] D.A. Cowan, R. Fernandez-Lafuente, Enzyme Microb. Technol. 49 (2011) 326–346.
[24] S. Chakraborti, T. Chatterjee, P. Joshi, A. Poddar, B. Bhattacharyya, S.P. Singh, V. Gupta, P. Chakrabarti, Langmuir: ACS J. Surf. Colloids 26 (2010) 3506–3513.
[25] C. Yi, C.C. Fong, Q. Zhang, S.T. Lee, M. Yang, Nanotechnology 19 (2008) 095102.